ADV MATH SCI JOURNAL
Advances in Mathematics: Scientific Journal **9** (2020), no.11, 9187–9200
ISSN: 1857-8365 (printed); 1857-8438 (electronic)
https://doi.org/10.37418/amsj.9.11.24 Spec. Iss. on ICMMSIS-2020

NATURAL CONVECTION IN A MICROPOLAR NANOFLUID FILLED OPEN RECTANGULAR ENCLOSURE EMBEDDED WITH A HEATED OBJECT OF DIFFERENT GEOMETRIES

ENDALKACHEW GETACHEW USHACHEW[1] AND MUKESH KUMAR SHARMA[2]

ABSTRACT. A numerical investigation has been performed to analyze heat convection through a micropolar nanofluid in an open rectangular enclosure. It embedded the inner heated object of different geometries and finite heat source length on the bottom wall with uniform heat flux. The remaining portion of the wall containing heat source and all the remaining walls are assumed as adiabatic except the top wall. Successive over-relaxation (SOR) method coupled with Gauss-Seidel iteration technique are employed in order to numerically tackled the nonlinear model momentum and energy equations. The effect of the calibrated parameters such as Rayleigh number, length of the wall heat source, the geometry of the inner block, vortex viscosity parameter, the type of nanoparticles, and the concentration of nanoparticles on the flow and thermal performance is studied. The computed results show that increasing in the Rayleigh number and the concentration of nanoparticles have a positive effect on Nusselt number whereas increasing in wall heat source length and vortex viscosity attenuates the Nusselt number. Also, the geometry of the inner block has effect in the flow pattern and the temperature distribution.

1. INTRODUCTION

The sustainable enhancement of heat convection in thermal engineering without using excessive energy has been the demand of time. This enhancement,

[1]*corresponding author*

2020 *Mathematics Subject Classification.* 76A05.

Key words and phrases. Micropolar fluid, embedded heated object, open enclosure, nanofluid.

either in cooling or heating mechanism can be achieved by natural convection and has its own practical applications in industries, optimum use of solar energy, electronic cooling systems, nuclear energy, etc. However, this enhancement on heat exchangers can be determined by the thermal conductivities of the heat transfer fluid and the geometry of the heat exchangers. Among the heat transfer fluids, heat convection in nanofluids have got a great attention by researcher's because of its excellent thermal performance potential in heat transfer and its wide practical applications in industries. Nanofluid, a name conceived by Choi (1995), is a heat transfer fluid containing nanosized particles called nanoparticles. Studies showed that the addition of nanoparticles in common base fluids changes their thermophysical properties and increases their thermal conductivity. As noticed from the review done by Hosseini et al. (2011), the enhancement of nanofluids depends on several factors such as shape, size, volume fraction, temperature and thermal conductivities of nanoparticles, and the base fluids. The findings of numerical investigation on effect of a centred, square, heat conducting body on natural convection heat transfer in an enclosure by House et al. (1990) showed that the heat transfer across the enclosure might be enhanced or reduced by a body with a thermal conductivity ratio. The numerical investigation done by Pallab et al. (2013) on the heat transfer enhancement and entropy generation in square enclosure in the presence of adiabatic and isothermal blocks found that the heat transfer increases with increase of block size depending on the value of Rayleigh number. Roy (2019) analyzed the effect of a wavy-walled obstacle on heat convection through Al2O3-H2O nanofluid in a square enclosure.

On the other hand micropolar fluids have attracted attention as one of research area because of their importance in industries. The theory of micropolar fluid formulated by Eringen (1964;1966). The numerical investigation done by Aydin and Pop (2005) on natural convection from a discrete heater in enclosures filled with micro polar fluid obtained that micro polar fluids showed lower heat transfer values than those of the Newtonian fluids. The numerical investigation done by Rashad et al.(2017) on mixed convection from a discrete heater in lid driven enclosures filled with micropolar fluid nanofluids has been found that an increase in vortex viscosity parameter causes a reduction in Nusselt number . The study done by Sameh et al.(2018) on MHD mixed convection in trapezoidal enclosures filled with micropolar nanofluids shown that Hartmann number,heat

source location,and the dimensionless viscosity of the matterial have a siginificant effect on the average Nusselt number.

To the best of our knowledge, a detailed literature survey revealed that no attempt has been made to analyze the heat convection of micropolar Copper-water nanofluid filled rectangular open enclosure with finite length heat source at bottom wall and embedded heated object of different geometries. Thus, the purpose of this paper is to investigate numerically the heat convection in micropolar nanofluid filled rectangular open enclosure embeded with different inner geometries with respect to basic parametres such as Rayleigh number,vortex viscosity,volume of fraction of nanoparticles,types of nanoparticles, and length of wall heat source.

2. Problem formulation and Governing equations

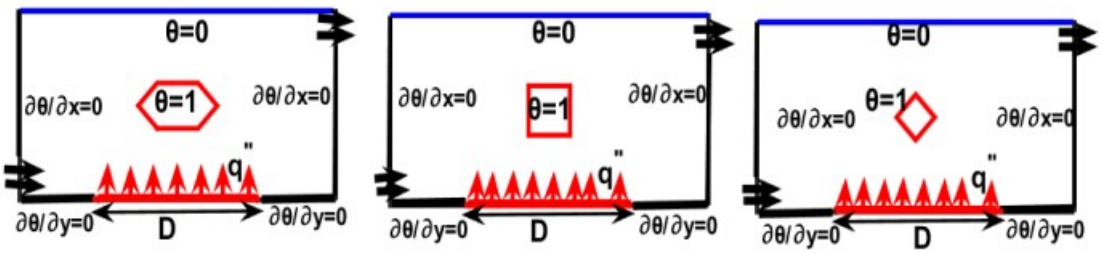

Figure 1. Problem Geometry

' The schematic diagram of the problem is as shown in the Fig.1. The length and height of an open rectangular enclosure are 2H and H, respectively. The open rectangular enclosure filled with a non-Newtonian fluid model called micropolar nanofluid.It contains an inner heated object of different geometries and finite heat source length on the bottom wall with a uniform heat flux.The remaining portion of the wall containing heat source and all the remaining walls are assumed as addiabatic except top wall.The top horizontal wall assumed as isothermally cold. The heated object is placed in the enclosure at equal distances from the horizontal and vertical walls of the enclosure. The inlet and outlet vent of width 0.1H are each taken at y=0 to y= 0.1H, on the left wall, and y=0.9H to y=H, on the right wall. The flow in the enclosure is assumed to be steady and laminar.The thermophysical properties of the nanofluid are

assumed constant except for density variation which is determined based on Boussinesq approximation.

Based on the above problem formulations and physical geometry, the governing equations for a micropolar nanofluid flow continuity, linear momentum, angular momentum and energy equations can be wrritten as follows in the dimensionless form.

$$\frac{\partial u}{\partial x}+\frac{\partial v}{\partial y}=0 \tag{2.1}$$

$$\begin{aligned} u\frac{\partial u}{\partial x}+v\frac{\partial u}{\partial y}=&-\frac{\partial p}{\partial x}+Pr(\frac{\rho_f}{\rho_{nf}})(\frac{\mu_{nf}}{\mu_f}+K)(\frac{\partial^2 u}{\partial x^2}+\frac{\partial^2 u}{\partial y^2})\\ &+PrK(\frac{\rho_f}{\rho_{nf}})(\frac{\partial N}{\partial y}) \end{aligned} \tag{2.2}$$

$$\begin{aligned} u\frac{\partial v}{\partial x}+v\frac{\partial v}{\partial y}=&-\frac{\partial p}{\partial y}+Pr(\frac{\rho_f}{\rho_{nf}})(\frac{\mu_{nf}}{\mu_f}+K)(\frac{\partial^2 v}{\partial x^2}+\frac{\partial^2 v}{\partial y^2})\\ &-PrK(\frac{\rho_f}{\rho_{nf}})(\frac{\partial N}{\partial x})+RaPr(\frac{\beta_{nf}}{\beta_f})\theta \end{aligned} \tag{2.3}$$

$$\begin{aligned} u\frac{\partial N}{\partial x}+v\frac{\partial N}{\partial y}=&Pr(\frac{\rho_f}{\rho_{nf}})(\frac{\mu_{nf}}{\mu_f}+\frac{K}{2})(\frac{\partial^2 N}{\partial x^2}+\frac{\partial^2 N}{\partial y^2})\\ &-PrK\chi(\frac{\rho_f}{\rho_{nf}})(2N-(\frac{\partial v}{\partial x}-\frac{\partial u}{\partial y})) \end{aligned} \tag{2.4}$$

$$u\frac{\partial \theta}{\partial x}+v\frac{\partial \theta}{\partial y}=\frac{\alpha_{nf}}{\alpha_f}(\frac{\partial^2 \theta}{\partial x^2}+\frac{\partial^2 \theta}{\partial y^2}) \tag{2.5}$$

The following dimensionless variables are introduced to obtain equations (2.1) to (2.5).

$x=\frac{x^*}{H}; y=\frac{y^*}{H}; u=\frac{u^*H}{\alpha_f}; v=\frac{v^*H}{\alpha_f}; p=\frac{p^*H^2}{\rho_{nf}\alpha_f^2}; \theta=\frac{T-T_{in}}{Hq^{''}}k_f; N=\frac{nH^2}{\alpha_f};$

$\chi=\frac{H^2}{j}; Pr=(\frac{\nu_f}{\alpha_{nf}})\ Prandtl\ number,\ Ra=\frac{gq^{''}\beta_f H^4}{\nu_f k_f}\ Rayleigh\ number\ ,$

$K=\frac{\kappa}{\mu_f}\ Vortex\ viscosity.$

The variables with asterisk $(*)$ denote dimensional variables. The subscripts nf and f symbolize the nanofluid and base fluid, respectively. In above equations u, v denotes the velocity of nanofluid along $x-, y-$ axis respectively, p is

pressure,μ is dynamic viscosity,ρ is density, α is thermal diffusivity, β is coefficient of volumetric thermal expansion, ϕ is concentration of nanoparticle and j is the microinertia density. The vorticity-stream function approach is implemented in order to remove the pressure term from the governing equations (2.2) and (2.3). Taking velocity components in terms of stream function Ψ as $u = \frac{\partial \psi}{\partial y}$; $v = -\frac{\partial \psi}{\partial x}$, and vorticity $\omega = \frac{\partial v}{\partial x} - \frac{\partial u}{\partial y}$ then Vorticity - stream function equation be

$$\frac{\partial^2 \Psi}{\partial x^2} + \frac{\partial^2 \Psi}{\partial y^2} = -\omega \tag{2.6}$$

$$\begin{aligned} u\frac{\partial \omega}{\partial x} + v\frac{\partial \omega}{\partial y} &= Pr(\frac{\rho_f}{\rho_{nf}})(\frac{\mu_{nf}}{\mu_f} + K)(\frac{\partial^2 \omega}{\partial x^2} + \frac{\partial^2 \omega}{\partial y^2}) \\ &\quad - PrK(\frac{\rho_f}{\rho_{nf}})(\frac{\partial^2 N}{\partial x^2} + \frac{\partial^2 N}{\partial y^2}) + RaPr(\frac{\beta_{nf}}{\beta_f})\frac{\partial \theta}{\partial x}. \end{aligned} \tag{2.7}$$

Angular momentum equation

$$\begin{aligned} u\frac{\partial N}{\partial x} + v\frac{\partial N}{\partial y} &= Pr(\frac{\rho_f}{\rho_{nf}})(\frac{\mu_{nf}}{\mu_f} + \frac{K}{2})(\frac{\partial^2 N}{\partial x^2} \\ &\quad + \frac{\partial^2 N}{\partial y^2}) - PrK\chi(\frac{\rho_f}{\rho_{nf}})(2N - \omega). \end{aligned} \tag{2.8}$$

Energy Equation

$$u\frac{\partial \theta}{\partial x} + v\frac{\partial \theta}{\partial y} = \frac{\alpha_{nf}}{\alpha_f}(\frac{\partial^2 \theta}{\partial x^2} + \frac{\partial^2 \theta}{\partial y^2}). \tag{2.9}$$

Density, thermal capacity, coefficient of thermal diffusivity, and volumetric expansion coefficient of nanofluid are computed by employing the expressions as defined in Pordanjani et al., 2018.

Maxwell (1973) model is taken to approximate thermal conductivity of nanofluid

$$\frac{k_{nf}}{k_f} = \frac{k_p + 2k_f - 2\phi(k_f - k_p)}{k_p + 2k_f + \phi(k_f - k_p)}. \tag{2.10}$$

The viscosity of nanofluid is taken as defined in the Brinkman (1952) model

$$\mu_{nf} = \mu_f \frac{1}{(1-\phi)^{2.5}}. \tag{2.11}$$

Based on the assumptions of the problem, the corresponding boundary conditions are considered as follows:

$\frac{\partial \theta}{\partial y} = -\frac{k_f}{k_{nf}}, u = v = 0\ at\ 0.75 \leq x \leq 1.25, y = 0$ and

$\frac{\partial \theta}{\partial y} = 0 \; at \; 0.0 \leq x < 0.75, y = 0 \; and \; 1.25 < x \leq 2.0, y = 0$ of the bottom wall

$\frac{\partial \theta}{\partial x} = 0, u = 0 = v; N = 0$ at left and right walls of the enclosure

$u = v = 0; N = \theta = 0$ at top wall of the enclosure

$u = 0; v = 0; \; and \; \theta = 1$ at the wall of inner block

$u = 1; v = 0; \theta = 0$ at the inlet $\frac{\partial u}{\partial x} = 0; \frac{\partial v}{\partial x} = 0; \frac{\partial \omega}{\partial x} = 0; \frac{\partial N}{\partial x} = 0; \frac{\partial \theta}{\partial x} = 0$ at the outlet

The local variation of the Nusselt number at heated portion of bottom wall can be calculated by using the expression

$$Nu = \frac{1}{\theta(x)}. \tag{2.12}$$

3. Method of Solution

Finite difference discretization approach is implemented to discritize governing equations from (2.6)-(2.9) with associated boundary conditions. Second order central and upwind differencing formulas are used in approximating diffusion and convective terms respectively, in the above equations. SOR method for stream function, under relaxation for vorticity and micro-rotation, and Gauss-Seidel iteration method for energy equation is implemented. The convergence criterion for Ψ, ω and θ is defined by $\frac{\Sigma_{i,j}|\Phi_{i,j}^{k+1} - \Phi_{i,j}^{k}|}{\Sigma_{i,j}|\Phi_{i,j}^{k+1}|} \leq 10^{-5}$ where Φ represents any of computed value of Ψ, ω and θ.

A MATLAB programme was built to execute the numerical algorithm for discretized governing equations. The computational MATLAB codes are validated with the findings of Bakar et al. (2016) as presented in Table 1, Jani et al. (2013) in figure 2. (a) for $Ra = 10^3$ in terms of streamlines and isotherms.

4. Results and discussion

The result of a numerical study of heat convection in micro polar nanofluid filled rectangular open enclosure with embedded heated object of different geometries is discussed in this section. The computations employed for Rayleigh number ranging from 10^3 to 10^5,Prandtl number 6.8, heat source length (D)

TABLE 1. Nusselt number on heated wall at Ri=1.0, Ha=60, Re=100

Size of grids	in Bakar et al	Present study
61 × 61	1.26228	1.2420
81 × 81	1.27974	1.2462
101 × 101	1.28140	1.2747
121 × 121	1.29458	1.2763
141 × 141	1.31062	1.2775

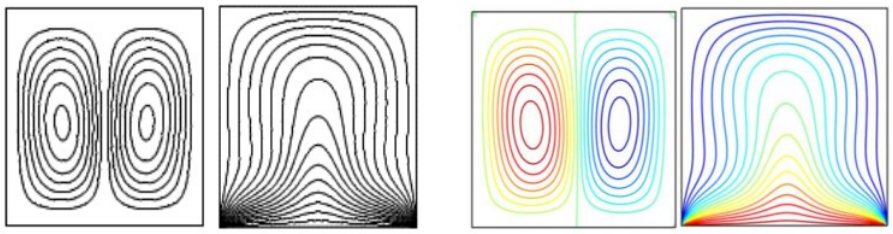

(a) Jani *et al*. (2013) (b) present study

FIGURE 2. Streamlines and Isotherms graph comparison for present study with Jani et al. (2013).

from 0.5H to 1.5H, volume fraction from 0 to 0.04 and vortex viscosity (K) ranging from 0.5 to 5. The analysis of governing parameters illustrated by Streamlines, Isotherms, Isolines and Nusselt number profiles. Based on the analysis of governing parameters, the results presented and discussed as follows.

The effects of bottom wall central heat source length on flow pattern and temperature distribution in the enclosure depicted by streamline and isotherms graph of figure 3. It is noticed from the streamline graph of figure 3(a) that the strength of circulation increases as the increase of heat source length. This is because of higher heat generation rate created from the increase of heat source length associated with stronger buoyant forces which magnify the strength of streamlines in the enclosure. Also, the size and the number of vortices changed as the increase of heat source length. The flow pattern noticed by symmetrical vortices in the left and right, top of inner block for all heat source lengths but the size of vortices various non-linearly as the increase of heat source length. The main reason for occurrence of symmetrical flow in the enclosure is due to the constant location of heat source. It is observed from isotherm graph 3(b) that

the size of non-isothermal regions reduced as the increase of heat source length. The isotherm lines concentrated to heat source location. Also, the strength of isotherms in the vicinity of heat source increased as the increase of the length of heat source. This is because of increase in length of heat source increases heat generation and hence increases the temperature at the surface of heat source. It is obvious to predict the Nusselt profile from equation 2.12 that increasing heat source length causes the Nusselt number to decrease.

To illustrate the effect of vortex viscosity of the material parameter on the selected geometry and the proposed problem streamlines, isotherms, isolines and Nusselt profiles are used from figure 4 to 5.Stream line graph of figure 4(a) shows that as the value of K increases the strength of the circulation becomes diminished and hence scattered streamlines observed. This because of that increasing vortex viscosity parameter of the material retards the fluid flow pattern and hence poor convection occurred. From figure 4(b) of isotherms graph as the value of K increases leads to the slight increase in the size of the portion of non-isothermal regions and increase in the strength of the isotherms contours in the vicinity of the wall heat source. This indicates weak heat transfer rate from heated wall to the fluid. From the isolines graph of 4(c) we can observe that increase in the value of K yields increases strength of the circulation and reduces the size of strong right micro-rotation in the enclosure. Increasing the value of K yields the disappearance of micro rotation cell near to two vertical walls. The local Nusselt number profile at the surface of wall heat source depicted by figure 5 and shows that increase in the value of vortex viscosity results decrease in the local Nusselt number. This indicates that increasing of the material parameter retards the heat transfer in the enclosure.

From the streamline graph of figure 6(a) shows that there is an increased intensity, compactness and number of vortex as the Rayleigh number increased. Also, it is observed that the shape of the core of circulating cell changed as the Rayleigh number increased. The increase in the value of Rayleigh number from $Ra = 10^3$ to $Ra = 10^4$, the buoyancy assistance to flow increases hence stronger vortex cell is developed. Further, increase in Rayleigh number to 10^5, rises the number of vortex cells and increases their strength. The main reason for the increase of intensity and number of circulating cells with the Ra is to overcome the viscous effect by the buoyancy effect. The temperature contour of the isotherm graph of figure 6(b) shows that clustered isotherms observed

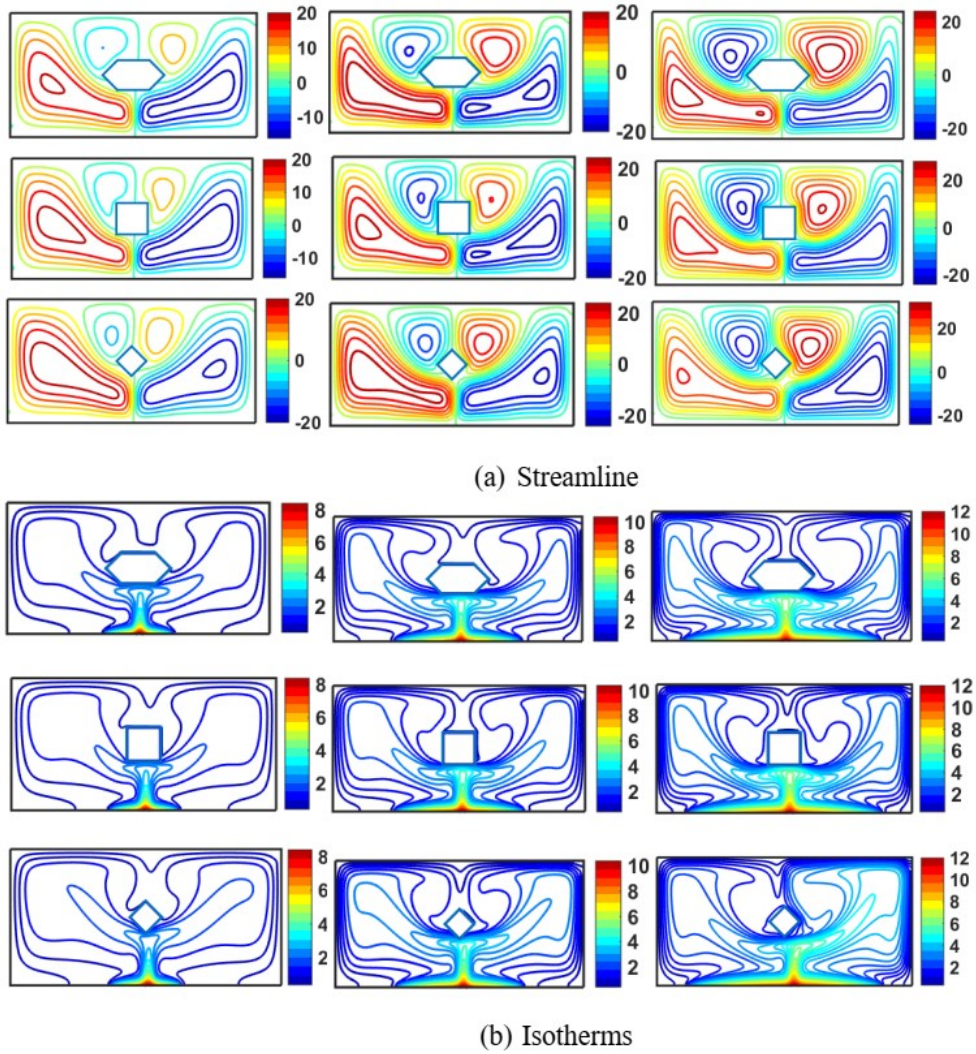

FIGURE 3. Streamline and Isotherms graph of different length (D=0.5H,1H and 1.5H) of middle of bottom wall heat source at $Ra = 10^5$, $\phi = 0.04$, Pr=6.8.

near to heat source and cold wall as Rayleigh number increased. Conduction dominated heat transfer flow noticed at $Ra = 10^3$ because of viscous dominancy at low Rayleigh number. The distortions of isotherms increased as the increase of the Rayleigh number. Diminished strength of isotherms observed from the vicinity of heat source as the increase of Rayleigh number. Moreover, the isotherms lines become more distorted with further increase in Rayleigh

number to $Ra = 10^5$ as a result of increasing of buoyancy force, the plumps of isotherms are heightened. This distortion shows an increased heat transfer at sufficiently high Rayleigh number and indicates intensification in the convective heat transfer. It is observed from local Nusselt profile of figure 7 that increase in Rayleigh boosts the Nusselt number. Thus, increase in Rayleigh number results increase in heat transfer in the enclosure. This effect is more pronounced in the enclosure embedding hexagon shape geometry.

The range of 0 to 0.04 copper nanoparticle volume fractions is used to deal its effect numerically on the fluid flow and thermal distribution in the proposed problem. Local Nusselt number profile at the heat source of figure 8 indicates that there is positive relationship between Nusselt number and volume fraction of nanoparticles. It indicates that convection of heat in a heat exchanger can be enhanced without altering the heat transfer fluid but by adding a small volume fraction of nanoparticles in it. The reason for this behaviour is due to the increase in the thermal conductivity. An enclosure with hexagon shape has better heat enhancement as the increase of concentration of nanoparticles.

To examine the influence of types of nanoparticles in the enclosure copper, silver and aluminium oxide with water as base fluid considered and the results disclosed by Nusselt profile of figure 9. It is noticed from local Nusselt number on the surface of heat source that Copper water nanofluid has the largest Nusselt number where as aluminium oxide has the lowest local Nusselt number. Thus, Copper water nanofluid has the highest heat transfer rate than silver water and aluminium oxide water nanofluid.

5. CONCLUSION

The computed results presented by streamline, isotherms, isolines, and local Nusselt profile graphs and analysed. Based on the results of the analysis the following conclusions are drawn.

- Increasing Rayleigh number results increased heat transfer rate and reduced temperature for heat source. This effect is more pronounced for $Ra = 10^5$ and conduction dominated heat transfer observed at $Ra = 10^3$.
- The flow pattern and temperature distribution in the enclosure significantly affected by the length of heat source.

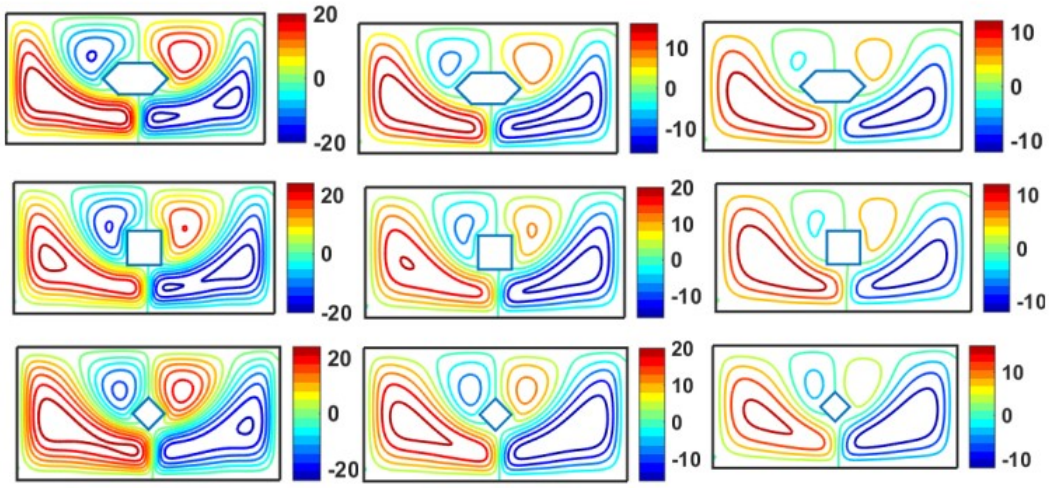

(a). streamline

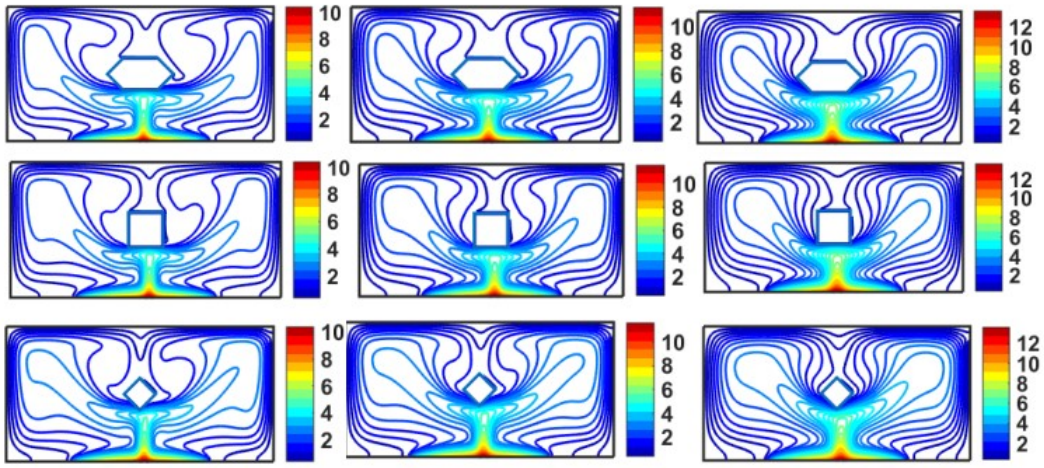

(b). Isotherms

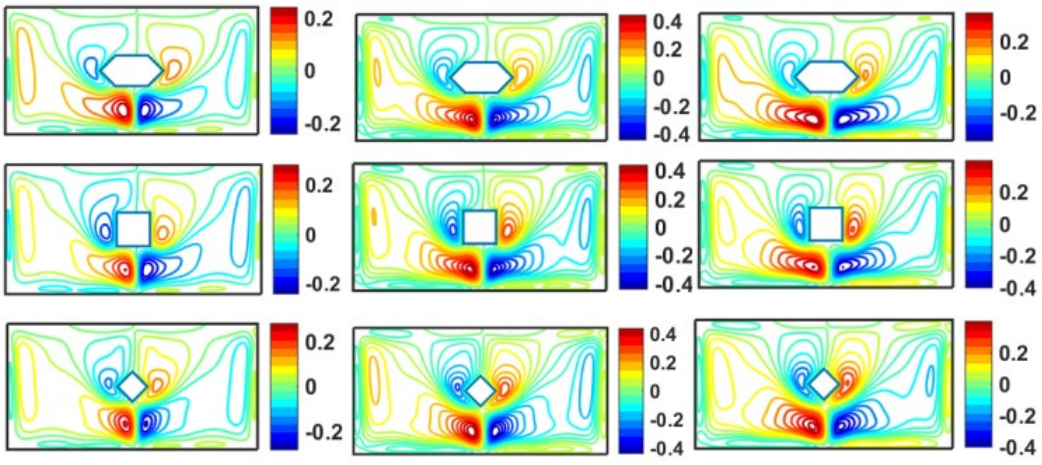

(c) Isolines

FIGURE 4. Streamline, Isotherms and Isolines graph of vortex viscosity $(K = 0.5, 2, 5)$ value at $Ra = 10^5$, $\phi = 0.04$, Pr=6.8.

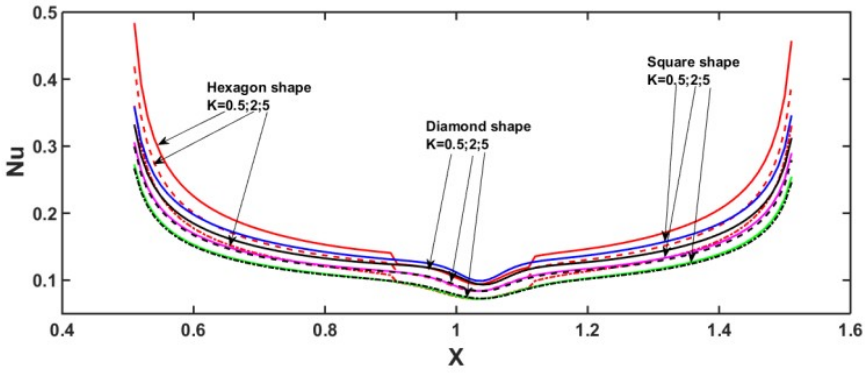

FIGURE 5. Local Nusselt number profile of different vortex viscosity at $Ra = 10^5$, Pr=6.8, $\phi = 0.04$.

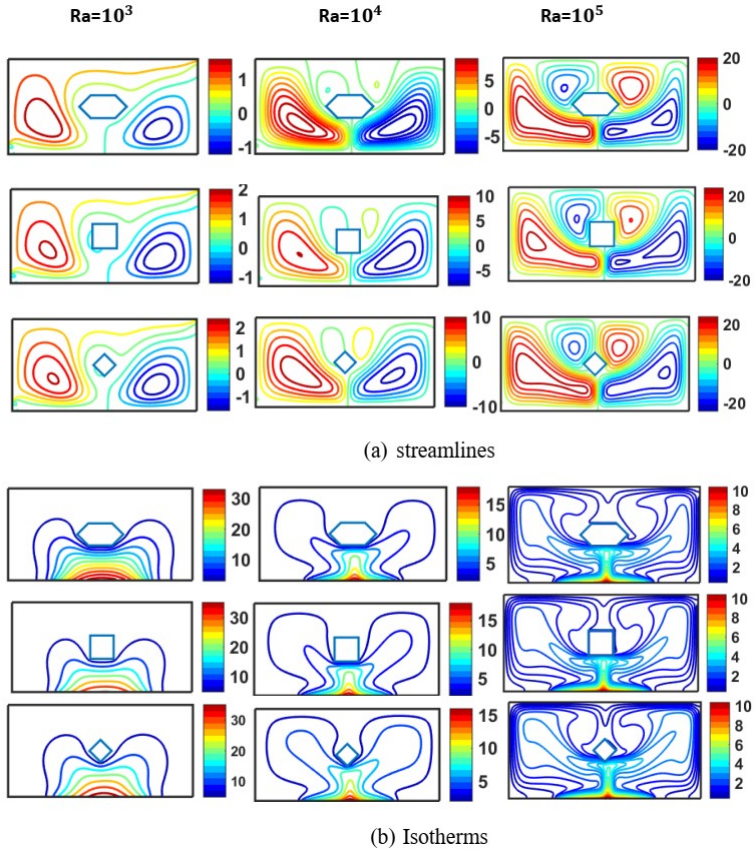

(a) streamlines

(b) Isotherms

FIGURE 6. Streamline and Isotherms graphs of different Rayleigh number at $\phi = 0.04$, Pr=6.8,K=0.5.

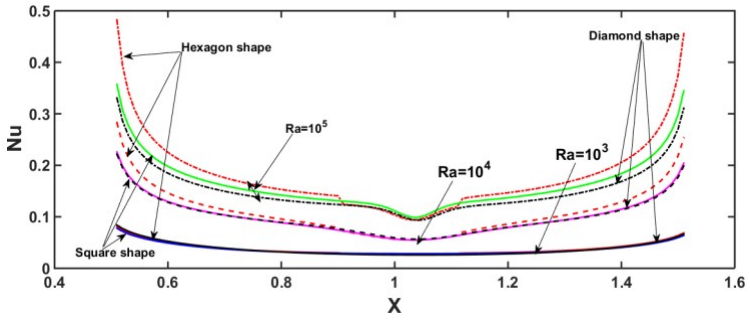

FIGURE 7. Local Nusselt number profile of different Rayleigh number at Pr=6.8, $\phi = 0.04$,K=0.5.

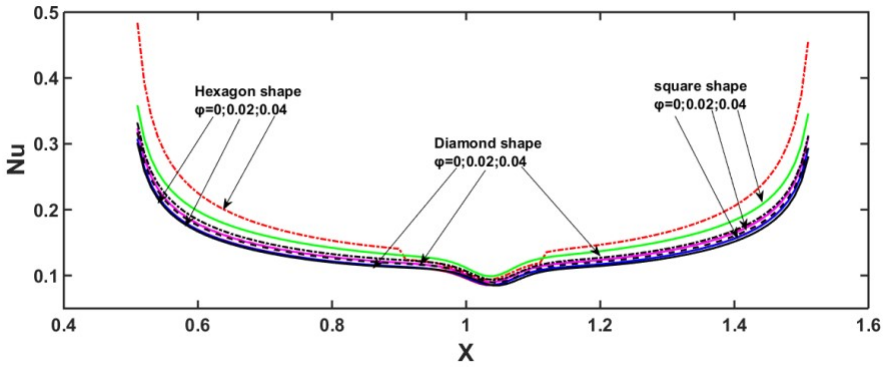

FIGURE 8. Local Nusselt number profile of different volume fraction at K=0.5, Pr=6.8, $Ra = 10^5$

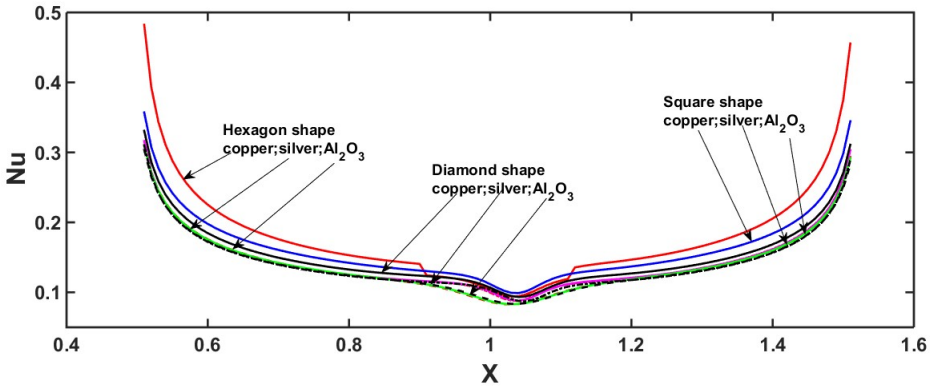

FIGURE 9. Local Nusselt number profile of different types of nanoparticles for K=0.5, Pr=6.8, $Ra = 10^5$

- Increasing in the value of vortex viscosity parameter of the micropolar fluid decreases heat transfer rate and hence decreases heat convection.
- Increasing volume of fraction of nanoparticles increases heat enhancement in the enclosure.
- Copper water nanofluid has highest heat transfer rate than silver water and aluminium oxide water nanofluid. Aluminium oxide water nanofluid has the lowest heat transfer performance.

REFERENCES

[1] S.U.S. CHOI: *Enhancing thermal conductivity of fluids with nanoparticles*, ASME Fluids Eng. Div., **231** (1995), 99–105.

[2] S.SH. HOSSEINI, A. SHAHRJERDI, Y. VAZIFESHENAS: *A Review of Relations for Physical Properties of Nanofluids*, Australian Journal of Basic and Applied Sciences, **5**(10) (2011), 417-435.

[3] J.M. HOUSE, C. BECKERMANN, T.F. SMITH: *Effect of a centred conducting body on natural convection heat transfer in an enclosure*, Numer. Heat Transfer, Part A, **18**(1990), 213-225.

[4] S. PALLAB, M.S. DE, K.G. NIRMAL, K. MANNA, A. MUKHOPADHYAY: *Heat transfer enhancement and entropy generation in a square enclosure in the presence of adiabatic and isothermal blocks*, Numerical Heat Transfer, Part A: Applications, **64**(7) (2013), 577-596.

[5] N.C. ROY: *Flow and heat transfer characteristics of a nanofluid between a square enclosure and a wavy wall obstacle*, Phys. Fluids. **31** (2019), art.id. 082005 .

[6] O. AYDIN, I. POP: *Natural convection from a discrete heater in enclosures filled with a micropolar fluid*, International Journal of Engineering Science, bf 43 (2005), 1409–1418.

[7] A.C. ERINGEN: *Simple micropolar fluids*, Int. J. Eng. Sci., bf 2(1964), 205–207.

[8] A.C. ERINGEN : *Theory of micropolar fluids*, J. Math. Mech., bf 16 (1966), 1–18.

[9] A.M. RASHAD, M.A. MANSOUR, R.S.R. GORLA: *Mixed convection from a discrete heater in lid-driven enclosures filled with non-Newtonian nanofluids*, J Nanomaterials, Nanoengineering and Nanosystems, bf 231(1) (2017), 3–16.

[10] S.E. AHMED, A.K. HUSSEIN, M.A. MANSOUR, Z.A. RAIZAH, X. ZHANG: *MHD mixed convection in trapezoidal enclosures filled with micropolar nanofluids nanoscience and technology*, An International Journal, bf 9(4) (2018), 343–372.

[1,2]DEPARTMENT OF MATHEMATICS, UNIVERSITY OF GURU JAMBHESHWAR UNIVERSITY OF SCIENCE AND TECHNOLOGY

HISAR,125001, INDIA

Email address: endalkgeta2001@gmail.com